

Full Length Article

Photocatalysis of composite film PDMS-PMN-PT@TiO₂ greatly improved via spatial electric field



Baoying Dai^{a,b,c}, Ling Zhang^{a,b,c}, Hengming Huang^{a,b,c}, Chunhua Lu^{a,b,c,*}, Jiahui Kou^{a,b,c,*}, Zhongzi Xu^{a,b,c}

^a State Key Laboratory of Materials-Oriented Chemical Engineering, College of Materials Science and Engineering, Nanjing Tech University, Nanjing 210009, PR China

^b Jiangsu Collaborative Innovation Center for Advanced Inorganic Function Composites, Nanjing Tech University, Nanjing 210009, PR China

^c Jiangsu National Synergetic Innovation Center for Advanced Materials (SICAM), Nanjing Tech University, Nanjing 210009, PR China

ARTICLE INFO

Article history:

Received 2 November 2016

Received in revised form

15 December 2016

Accepted 16 January 2017

Available online 17 January 2017

Keywords:

Piezoelectric effect

Photocatalysis

Film

PMN-PT

TiO₂

ABSTRACT

Efficient charge separation is quite significant to obtain high photocatalytic performance. In this work, piezoelectric-based composite photocatalyst film PDMS-PMN-PT@TiO₂ possessing high recoverability was prepared. The spatial electric field of PMN-PT was introduced into photocatalyst system by ultrasonic wave vibration to accelerate charge separation. Compared with magnetic stirring, ultrasonic wave vibration greatly improved the photocatalytic degradation efficiency of rhodamine B (RhB) over PDMS-PMN-PT@TiO₂ film by about 55%. A possible improvement mechanism that spatial electric field promotes charge separation was presented herein. The piezoelectric potential output demonstrated the piezoelectricity of composite film. The durability experiments of PDMS-PMN-PT@TiO₂ film indicated its great stability over several runs.

© 2017 Elsevier B.V. All rights reserved.

1. Introduction

Due to the development of industrialization, rapid pollution growth and long-term droughts, the shortage of clean water sources becomes a serious problem worldwide [1]. In addition, many organic waste pollutions which come from textile and other industrial processes are toxic and have a deleterious effect on the ecological environment [2,3]. Hence, the conversion of wastewater to harmless and readily disposable water is of importance for sustainable development. Photocatalysis, using semiconductor catalysts and ultraviolet light (UV) or visible light to degrade organic dyes into harmless substances [4], is activated by the absorption of a photon with sufficient energy equal or greater to the bandgap of catalyst. Photogenerated electrons and holes are separated and some of them transfer to the surface to take part in reduction and oxidation reaction, respectively [1]. However, many electrons and holes are recombined in the volume or on the surface of catalyst during photocatalysis. As we know, high carrier recombination

rate is one of the most important reasons for low photocatalytic efficiency. Though many modification methods based on charge separation have been proposed to improve photocatalytic efficiency [5–8], the enhancement effect is not good enough by now. Hence, it is imperative to explore a more efficient method to promote charge separation and achieve high photocatalytic performance.

Recently, the spatial electric field of piezoelectrics was introduced into photocatalytic system by applied force or thermal stress to improve photocatalytic activity [9–11]. It was concluded that higher piezoelectric effect of piezoelectrics is beneficial for achieving greater improvement effect. In the previous work, piezoelectrics with low piezoelectric effect resulted in poor charge separation effect and limited its enhancement role in photocatalysis. Therefore, lead magnesium niobate-lead titanate 0.675Pb(Mg_{1/3}Nb_{2/3})O₃-0.325PbTiO₃ (PMN-PT), possessing greater piezoelectric effect with a high d₃₃ of 2500 pm/V, should be constructed with photocatalyst and introduced into photocatalyst system [12,13]. Moreover, an inherent obstacle of powder photocatalyst is that it is difficult to recycle in the practical application. If the collection process of powder photocatalyst is mishandled, it will create more serious secondary pollution in the environment and the further treatment of stable photocatalyst will

* Corresponding authors at: State Key Laboratory of Materials-Oriented Chemical Engineering, College of Materials Science and Engineering, Nanjing Tech University, Nanjing, 210009, PR China.

E-mail addresses: chhlu@njtech.edu.cn (C. Lu), jhkou@njtech.edu.cn (J. Kou).

cost much. Therefore, photocatalyst films with easy accessibility and high recoverability needs to be developed urgently. Polydimethylsiloxane (PDMS), possessing excellent chemical stability, anti-ultraviolet ageing performance and thermostability, is generally used as substrate to prepare films and other devices [14,15]. The photocatalytic activity of titanium dioxide (TiO_2), with brilliant stability and efficient photocatalytic activity, has been reported and studied for nearly half a century. It is considered to be a promising and attractive photocatalyst for practical application [16–18].

In this paper, piezoelectric PMN-PT was constructed with TiO_2 to prepare piezoelectric-based composite photocatalyst PMN-PT@ TiO_2 . To avoid introducing secondary pollution into environment in the practical application, composite film PDMS-PMN-PT@ TiO_2 was fabricated. Furthermore, ultrasonic wave vibration was introduced into photocatalysis to compel PMN-PT to deform and generate spatial electric field to accelerate charge separation. The improvement mechanism of spatial electric field on photocatalytic activity was proposed. The piezoelectric potential output of PDMS-PMN-PT@ TiO_2 film was recorded with an oscilloscope to demonstrate its piezoelectricity. The stability of the composite film was also studied under the UV light irradiation and ultrasonic wave vibration.

2. Experimental

2.1. Materials

All the reagents were of analytical grade and were used without further purification. Distilled water was used in the whole experiment. Magnesium carbonate basic pentahydrate ($(\text{MgCO}_3)_4 \cdot \text{Mg}(\text{OH})_2 \cdot 5\text{H}_2\text{O}$, 40.0–44.5%), niobium ($\epsilon\delta$) oxide (Nb_2O_5 , 99.5%), trilead tetraoxide (Pb_3O_4 , 95.0%), titanium dioxide (TiO_2 , 98.0%) and ethanol ($\text{CH}_3\text{CH}_2\text{OH}$, 99.7%) were purchased from Sinopharm Chemical Reagent Co., Ltd to prepare piezoelectric PMN-PT powders. To synthesize nano titanium dioxide (TiO_2) sample, tetrabutyl titanate ($\text{Ti}(\text{OC}_4\text{H}_9)_4$, 98.0%) was purchased from Shanghai Lingfeng Chemical Reagent Co., Ltd. Poly(dimethylsiloxane) ($(\text{C}_2\text{H}_6\text{OSi})_n$, PDMS, Sylgard 184) and its curing agent from Dow Corning were used as film substrate. Xylene (C_8H_{10} , 99.0%, Shanghai Lingfeng Chemical Reagent Co., Ltd.) was used as the solvent of PDMS

2.2. Synthesis of photocatalytic powders

Nano TiO_2 particles were prepared via a simple hydrothermal method using tetrabutyl titanate, distilled water and ethanol as starting materials [19]. PMN-PT sample was synthesized by a conventional two-stage solid phase sintering method [20]. Piezoelectric-based composite photocatalyst PMN-PT@ TiO_2 was prepared through a hydrothermal process. The as-synthesized PMN-PT powders were mixed with tetrabutyl titanate, distilled water and ethanol and stirred for 30 min, then the mixture was transferred into a 100 mL homemade polytetrafluoroethylene (PTFE) lined stainless steel reactor and heated at 150°C for 24 h. After cooling down to room temperature, the target product was washed and centrifuged with ethanol for several times. Finally, the obtained powders were dried in an oven at 70°C overnight.

2.3. Preparation of composite films

To fabricate composite films, 0.6 g curing agent of PDMS was dispersed in 4.0 g xylene by ultrasonic for 10 min, and then 6.0 g PDMS was added and the mixture was stirred strongly for 30 min to form a homogeneous solution. After that, 1.0 g as-synthesized photocatalyst (TiO_2 or PMN-PT@ TiO_2) powders were added subsequently and violent stirring was maintained for 1 h. Ultrasonic

wave vibration was also introduced and maintained for 10 min to avoid catalyst powders agglomerating in the resins. Subsequently, the mixture was spin-coated on glass slides ($2.5\text{ cm} \times 7.6\text{ cm}$) with coating machine and cured at 70°C for 4 h in an oven. As last, the films with thickness about $100\ \mu\text{m}$ were peeled off. Pure PDMS film was also fabricated as well to compare the structure and optical properties with photocatalytic composite films.

2.4. Characterization

The phase structure characterization of the as-synthesized powders and films was performed on a SmartLab (Rigaku) thin-film diffractometer employing $\text{Cu K}\alpha$ radiation ($\lambda = 0.15406\text{ nm}$). Scanning electron microscopy (SEM) was performed with a S-4800 scanning electron analyzer with an accelerating voltage of 15 kV. The contact angles of the film samples were measured under ambient condition with a Contact Angle Analyzer (JGW-306). The sessile drop method was used to determine the contact angle. The UV-vis absorption spectra of the prepared samples were characterized by Ultraviolet-visible-near infrared (UV-vis-Nir) 3101 spectrophotometer (Shimadzu). The piezoelectric potential output signals were collected with an oscilloscope (Tektronic, DMO3024).

2.5. Photocatalytic performance evaluation

To estimate the photocatalytic activity of photocatalyst films and investigate the role of spatial electric field in photocatalysis, a 15 W lamp ($\lambda_{\text{max}} = 254\text{ nm}$) was used as UV light source, the distance between light source and reaction substance is about 20 cm. The ultrasonic wave vibration was introduced by a SK3300HP ultrasonic machine (Kedao) with the working frequency of 53 kHz and the consumed power of 180 W. Prior catalytic reaction, a piece of photocatalyst film was immersed in RhB solution and stirred for 1 h in dark to establish absorption-desorption equilibrium. The photocatalytic degradation experiments of RhB (12 mg/L, 90 mL) were carried out under ultrasonic wave vibration in the presence (U-L) and absence (U-NL) of UV light irradiation, magnetic stirring and UV light illumination (S-L), respectively. During all the catalytic process, any temperature rises were avoided by cool alcohol circulation. The photocatalytic stability of PDMS-PMN-PT@ TiO_2 film was investigated under U-L.

3. Results and discussion

Fig. 1 shows the XRD patterns of TiO_2 and PMN-PT@ TiO_2 powders, pure PDMS film, PDMS- TiO_2 and PDMS-PMN-PT@ TiO_2 composite films. The diffraction peaks of TiO_2 can be found at 25.4° , 38.0° , 48.1° , 54.8° and 62.9° , indexed as (101), (004),

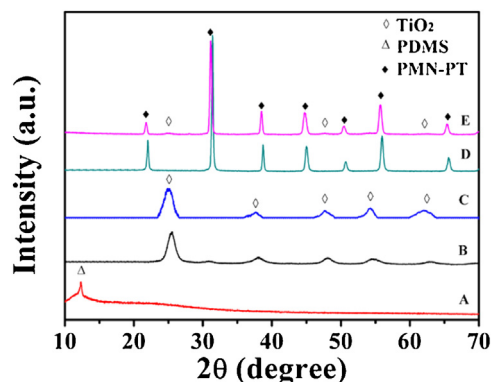


Fig. 1. XRD patterns of photocatalyst powders TiO_2 (B) and PMN-PT@ TiO_2 (D), and films PDMS (A), PDMS- TiO_2 (C) and PDMS-PMN-PT@ TiO_2 (E).

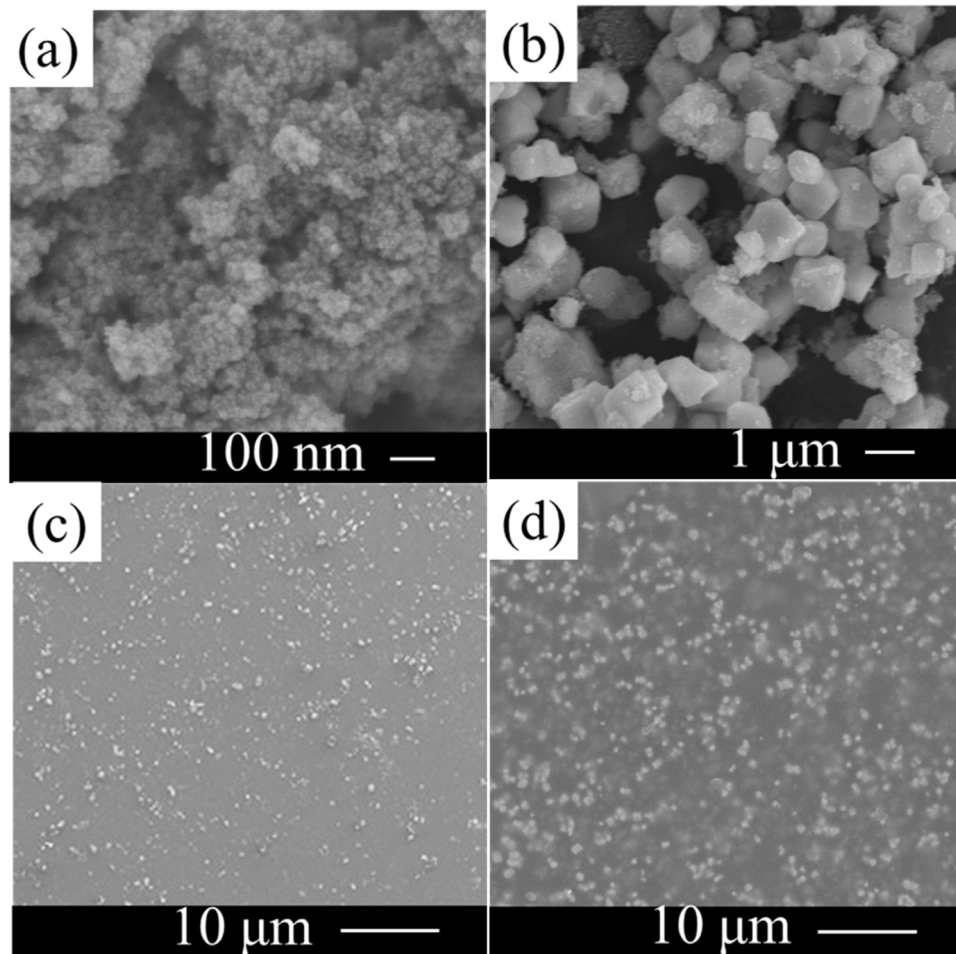


Fig. 2. SEM images of prepared TiO₂ (a), PMN-PT@TiO₂ (b) powders, PDMS-TiO₂ film (c) and PDMS-PMN-PT@TiO₂ film (d).

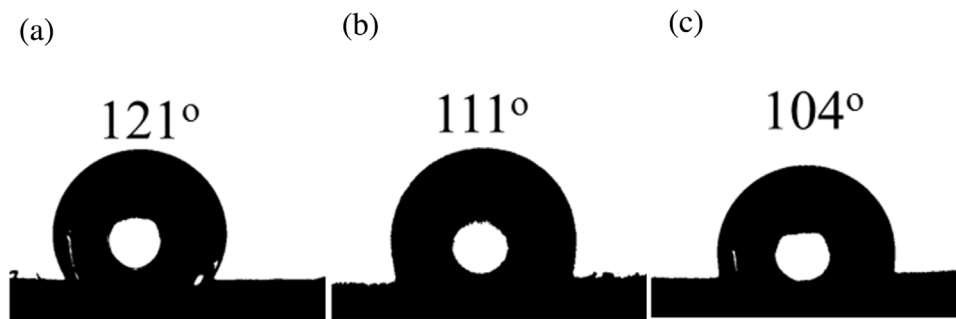


Fig. 3. The contact angles of the prepared PDMS film (a), PDMS-TiO₂ film (b) and PDMS-PMN-PT@TiO₂ film (c).

(200), (105) and (204) planes of anatase titanium dioxide, respectively. The peaks are in good agreement with the reported values [19,21,22]. All the strong peaks of PMN-PT@TiO₂ belong to pure perovskite structured PMN-PT with the lattice constants of $a = 4.03 \text{ \AA}$, $b = 4.00 \text{ \AA}$, and $c = 4.02 \text{ \AA}$, being consistent with the standard values of thin film PMN-PT [23]. It is attributed that the content of TiO₂ deposited on PMN-PT is too low to be detected. Furthermore, all the diffraction peaks of PDMS-TiO₂ and PDMS-PMN-PT@TiO₂ films belong to pure TiO₂ and PMN-PT@TiO₂ powders, respectively, implying that the phase structures of TiO₂ and PMN-PT@TiO₂ maintain well after introduced into PDMS substrate.

The SEM images of TiO₂ and PMN-PT@TiO₂ powders synthesized via hydrothermal method are displayed in Fig. 2 (a) and (b), respectively. The size of TiO₂ spherical particles is in nano scale.

TiO₂ particles are deposited on the surface of PMN-PT uniformly and tightly (Fig. 2 (b)). Fig. 2 (c) and (d) suggest that TiO₂ and PMN-PT@TiO₂ particles are relatively uniformly distributed around the surface of PDMS substrate, respectively. It should be pointed out that some photocatalyst particles agglomerate together with the size less than 1 μm. It is ascribed to the solvent evaporation and volume contraction of the reaction mixture during the curing process.

Surface wetting property is always being used to characterize the surface chemical composition, surface free energy and surface morphology [18,24,25]. To further demonstrate that TiO₂ and PMN-PT@TiO₂ particles are exposed on the surface of prepared films, therefore, the contact angles of the liquid droplet on the surface of pure PDMS, PDMS-TiO₂ and PDMS-PMN-PT@TiO₂ composite films

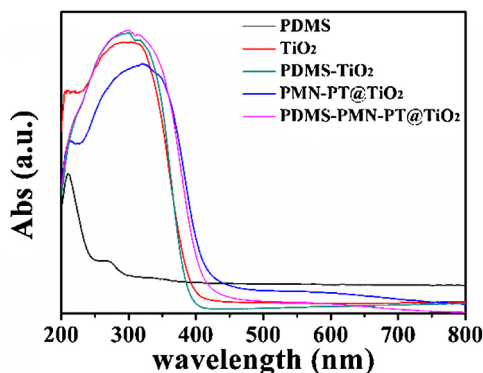


Fig. 4. The UV–vis absorption spectra of TiO_2 , PMN-PT@ TiO_2 powders, PDMS, PDMS- TiO_2 and PDMS-PMN-PT@ TiO_2 films.

were measured, respectively. As Fig. 3 shows, the contact angle of pure PDMS film is 121° , after mixed with TiO_2 , the angle decreases to 111° (Fig. 3 (b)). The contact angle of PDMS-PMN-PT@ TiO_2 film is 104° . PDMS- TiO_2 and PDMS-PMN-PT@ TiO_2 composite films exhibit a smaller contact angle than pure PDMS film, respectively, providing a powerful demonstration that some TiO_2 and PMN-PT@ TiO_2 particles are exposed on the surface of PDMS substrate.

Fig. 4 displays the UV–vis absorption spectra of the prepared samples. The obvious photo-absorption of TiO_2 powders starts at 400 nm, which corresponds to the band gap of 3.10 eV. The UV–vis absorption edge of PMN-PT@ TiO_2 sample is around 420 nm, indicating a little red-shift compared with TiO_2 . It is ascribed to the construction with PMN-PT. Pure PDMS film exhibits few absorption in the wavelength ranged from 200 nm to 800 nm. It suggests that PDMS, utilized as photocatalyst film substrate, does not influence the optical property of photocatalyst. It is further confirmed by the absorption edges of PDMS- TiO_2 and PDMS-PMN-PT@ TiO_2 composite films which are similar to that of TiO_2 and PMN-PT@ TiO_2 powders, respectively.

To obtain the potential signals of PDMS- TiO_2 and PDMS-PMN-PT@ TiO_2 films, a turbo-dynamo with the frequency of 50 Hz was introduced to deform the prepared film, and the generated piezoelectric potential output signals were recorded with an oscilloscope. As Fig. 5 shows, almost no potential signal is recorded over PDMS- TiO_2 film, the reason is that both PDMS and TiO_2 do not possess piezoelectric property. The piezoelectric potential of PDMS-PMN-PT@ TiO_2 film (Fig. 5 (b)) is varied periodically from -2.5 V to $+2.5\text{ V}$ with a period of 0.02 s, corresponding to the frequency of 50 Hz. It indicates that the piezoelectric property of the prepared PDMS-PMN-PT@ TiO_2 film is pretty good, and the film is quite sensitive to the applied force. Moreover, it can be

reasonably inferred that the piezoelectric potential of PDMS-PMN-PT@ TiO_2 film will generate periodically with a high frequency under ultrasonic wave vibration. In essence, this kind of generated piezoelectric potential is an alternative spatial electric field.

Fig. 6 depicts the photodegradation capability on RhB over the prepared films PDMS- TiO_2 and PDMS-PMN-PT@ TiO_2 under U-L, S-L and U-NL, respectively. As Fig. 6 (a) shows, the adsorption test was pre-conducted in dark for 1 h and then degradation proceeded at $t=0$. The adsorption test results showed that the adsorption-desorption equilibrium has been reached, the adsorption of RhB under each condition could be neglected in the presence of ultrasonic wave and/or light irradiation. The degradation efficiency of RhB catalyzed over PDMS- TiO_2 (40%) is slightly higher than that over PDMS-PMN-PT@ TiO_2 film (35%) under S-L, indicating that the photocatalytic activity of PDMS- TiO_2 is prior to that of PDMS-PMN-PT@ TiO_2 . About 90% of RhB has been converted by PDMS-PMN-PT@ TiO_2 film in the presence of ultrasonic wave vibration and UV light irradiation, which is much higher than that converted by PDMS- TiO_2 film (less than 65%). It suggests that the photocatalytic activity of PDMS- TiO_2 is worse than PDMS-PMN-PT@ TiO_2 under U-L. This result is against with that under S-L. Moreover, there is no obvious difference in the degradation efficiency of RhB over PDMS- TiO_2 and PDMS-PMN-PT@ TiO_2 films under U-NL. It demonstrates that the role of ultrasonic wave vibration on the photocatalytic activity of PDMS- TiO_2 and PDMS-PMN-PT@ TiO_2 films is not the same. To better compare the photocatalytic performance of two films, the photodegradation efficiencies of PDMS- TiO_2 and PDMS-PMN-PT@ TiO_2 under the above three mentioned conditions in 4 h are displayed in Fig. 6 (b). The photocatalytic efficiencies of PDMS- TiO_2 and PDMS-PMN-PT@ TiO_2 films are improved by about 25% and 55% under U-L, compared with that under S-L, respectively. While only 14% and 20% of RhB were degraded over PDMS- TiO_2 and PDMS-PMN-PT@ TiO_2 films under U-NL, respectively. It indicates that the ultrasonic wave vibration itself is not the reason for the difference in the enhancement effect of ultrasonic wave vibration on photocatalytic performance. Taking the difference in piezoelectric potential output of PDMS- TiO_2 and PDMS-PMN-PT@ TiO_2 films into account, it is necessary to analyze the synergistic effect of UV light illumination and ultrasonic wave vibration on photocatalytic activity.

As Scheme 1 displays, PDMS-PMN-PT@ TiO_2 film (Scheme 1 (a)) suffers the irradiation of UV light and ultrasonic wave. Take a small part as example (Scheme 1 (b)), about 1000 atmospheres pressure, generated by acoustic cavitation phenomenon [11], deforms the piezoelectric powder PMN-PT (Scheme 1 (c)), positive and negative piezoelectric potentials are generated respectively on the opposite surfaces of PMN-PT simultaneously. With UV light irradiation, the photogenerated electrons (black spheres) and holes (pink spheres)

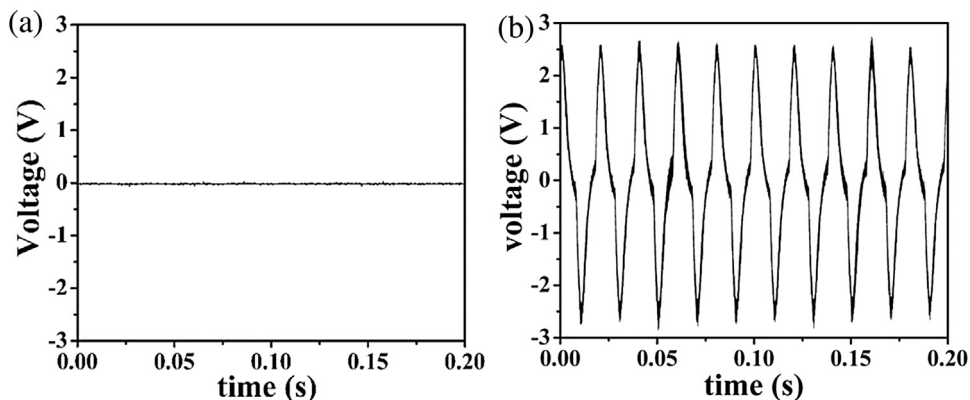


Fig. 5. The potential outputs of PDMS- TiO_2 film (a) and PDMS-PMN-PT@ TiO_2 film (b) under applied force.

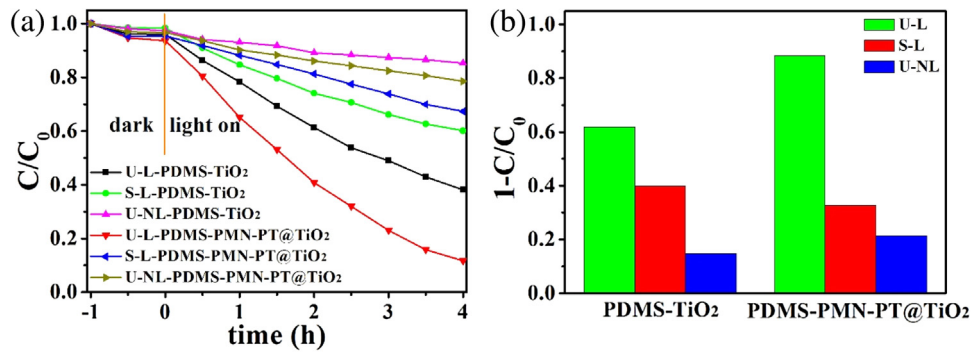
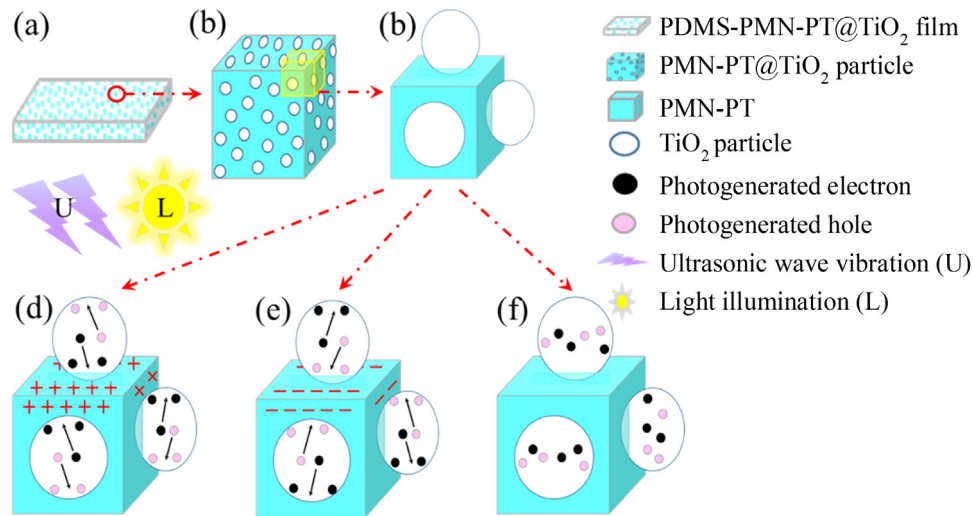


Fig. 6. The photodegradation curves of RhB (12 mg/L, 90 mL) catalyzed by PDMS-TiO₂ and PDMS-PMN-PT@TiO₂ films under U-L, U-NL and S-L (a), the degradation efficiency of RhB in 4 h under U-L, S-L and U-NL (b).



Scheme 1. The schematic of photocatalytic efficiency enhanced by the spatial electric field of PMN-PT. PDMS-PMN-PT@TiO₂ film (a), PMN-PT@TiO₂ particle (b), a small part of PMN-PT@TiO₂ particle (c), positive (d) and negative (e) potential emerge on the surfaces of PMN-PT, piezoelectric potential disappears (d).

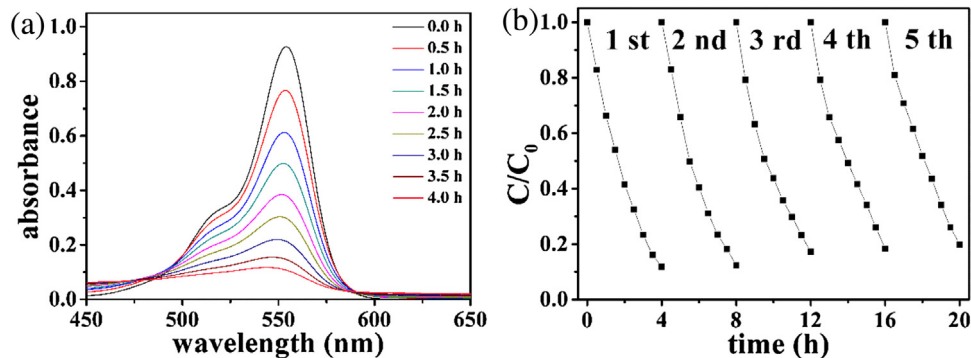


Fig. 7. The UV-vis absorption spectra (a) and cyclic degradation curves (b) of RhB over PDMS-PMN-PT@TiO₂ film under U-L.

of TiO₂ (white particles) are excited and directly transfer to the positive and negative piezoelectric potential surfaces of PMN-PT (blue cube) driven by spatial electric field, respectively, described in Scheme 1 (d) and (e). As a result, the recombination of the carriers is restricted. When piezoelectric potential turns zero, as Scheme 1 (f) depicts, the photogenerated carriers of TiO₂ moves randomly, and the charge separation is no longer accelerated. It should be pointed out that, as Fig. 5 indicates, the time corresponding to zero potential is quite short and even could be ignored. Therefore, the charge separation is promoted by spatial electric field during almost the whole photocatalytic process and the photocatalytic activity is enhanced

by about 55%. As for PDMS-TiO₂ film, no piezoelectric potential is generated and the carriers move freely under U-L, the charge separation is not promoted, the photocatalytic activity of PDMS-TiO₂ is not improved much.

The durability experiment of PDMS-PMN-PT@TiO₂ film was carried out under ultrasonic wave vibration and UV light irradiation. There is few decrease in catalytic activity of the film after five runs, as Fig. 7 displays, indicating the excellent photocatalytic stability of PDMS-PMN-PT@TiO₂. Moreover, the degradation activity of RhB under U-L is maintained well over every run. It suggests that the periodically generated spatial electric field of PMN-PT

accelerates the separation of the photogenerated carriers of TiO₂ throughout the whole photocatalytic process. It also demonstrates the piezoelectric stability and sensitivity of PMN-PT. Furthermore, the fabrication of photocatalyst film makes the reclaim of photocatalyst easier in the practical application, which avoids introducing secondary pollution into environment.

4. Conclusion

In summary, piezoelectric-based composite photocatalyst PDMS-PMN-PT@TiO₂ film was prepared. The spatial electric field of PMN-PT was introduced via ultrasonic wave vibration, which highly improves the photocatalytic efficiency of PDMS-PMN-PT@TiO₂ by about 55%. The durability experiment suggests that PDMS-PMN-PT@TiO₂ film keeps excellent stability even after five runs. In a wider perspective, this work provides a new strategy coupling mechanical energy and solar energy to greatly enhance photocatalytic performance, the preparation of photocatalyst film avoids introducing secondary pollution into environment in the practical application.

Acknowledgements

Financial support from National Natural Science Foundation of China (Nos. 51303079, 51502143), Natural Science Foundation of Jiangsu Province (Nos. BK20141459, BK20150919), Qing Lan Project, Six Talent Peaks Project in Jiangsu Province (No. XCL-029), Project on the Integration of Industry, Education and Research of Jiangsu Province (No. BY2015005-16), Key University Science Research Project of Jiangsu Province (No. 15KJB430022) and Priority Academic Program Development of the Jiangsu Higher Education Institutions (PAPD) is gratefully acknowledged.

References

- [1] W. Wang, M.O. Tade, Z. Shao, Research progress of perovskite materials in photocatalysis- and photovoltaics-related energy conversion and environmental treatment, *Chem. Soc. Rev.* 44 (2015) 5371–5408.
- [2] N. Cheng, J. Tian, Q. Liu, C. Ge, A.H. Qusti, A.M. Asiri, A.O. Al-Youbi, X. Sun, Au-nanoparticle-loaded graphitic carbon nitride nanosheets: green photocatalytic synthesis and application toward the degradation of organic pollutants, *ACS Appl. Mater. Interface* 5 (2013) 6815–6819.
- [3] P. Singh, K. Mondal, A. Sharma, Reusable electrospun mesoporous ZnO nanofiber mats for photocatalytic degradation of polycyclic aromatic hydrocarbon dyes in wastewater, *J. Colloid Interface Sci.* 394 (2013) 208–215.
- [4] M.F.Y.W. Hongbao Yao, Magnetic titanium dioxide based nanomaterials: synthesis, characteristics, and photocatalytic application in pollutant degradation, *J. Mater. Chem. A* 3 (2015) 17511–17524.
- [5] X. Bai, R. Zong, C. Li, D. Liu, Y. Liu, Y. Zhu, Enhancement of visible photocatalytic activity via Ag@C₃N₄ core-shell plasmonic composite, *Appl. Catal. B: Environ.* 147 (2014) 82–91.
- [6] S. Ramadurgam, T. Lin, C. Yang, Aluminum plasmonics for enhanced visible light absorption and high efficiency water splitting in core-multishell nanowire photoelectrodes with ultrathin hematite shells, *Nano Lett.* 14 (2014) 4517–4522.
- [7] T. Hirakawa, P.V. Kamat, Charge separation and catalytic activity of Ag@TiO₂ core-shell composite clusters under UV-irradiation, *J. Am. Chem. Soc.* 127 (2005) 3928–3934.
- [8] T.W. Kim, S.G. Hur, S.J. Hwang, H. Park, W. Choi, J.H. Choy, Heterostructured visible-light-active photocatalyst of chromia-nanoparticle-layered titanate, *Adv. Funct. Mater.* 17 (2007) 307–314.
- [9] L. Wang, S. Liu, Z. Wang, Y. Zhou, Y. Qin, Z.L. Wang, Piezotronic effect enhanced photocatalysis in strained anisotropic ZnO/TiO₂ nanoplatelets via thermal stress, *ACS Nano* 10 (2016) 2636–2643.
- [10] X. Xue, W. Zang, P. Deng, Q. Wang, L. Xing, Y. Zhang, Z.L. Wang, Piezo-potential enhanced photocatalytic degradation of organic dye using ZnO nanowires, *Nano Energy* 13 (2015) 414–422.
- [11] H. Li, Y. Sang, S. Chang, X. Huang, Y. Zhang, R. Yang, H. Jiang, H. Liu, Z.L. Wang, Enhanced ferroelectric-nanocrystal-based hybrid photocatalysis by ultrasonic-wave-generated piezophototronic effect, *Nano Lett.* 15 (2015) 2372–2379.
- [12] S. Xu, Y. Yeh, G. Poirier, M.C. McAlpine, R.A. Register, N. Yao, Flexible piezoelectric PMN-PT nanowire-based nanocomposite and device, *Nano Lett.* 13 (2013) 2393–2398.
- [13] S. Xu, G. Poirier, N. Yao, Fabrication and piezoelectric property of PMN-PT nanofibers, *Nano Energy* 1 (2012) 602–607.
- [14] N. Nama, R. Barnkob, Z. Mao, C.K. Hler, F. Costanzo, Numerical study of acoustophoretic motion of particles in a PDMS microchannel driven by surface acoustic waves, *Lab Chip* 15 (2015) 2700–2709.
- [15] I. Babu, G. de With, Highly flexible piezoelectric 0-3 PZT-PDMS composites with high filler content, *Compos. Sci. Technol.* 91 (2014) 91–97.
- [16] M. Liu, R. Inde, M. Nishikawa, X. Qiu, D. Atarashi, E. Sakai, Y. Nosaka, K. Hashimoto, M. Miyauchi, Enhanced photoactivity with nanocluster-grafted titanium dioxide photocatalysts, *ACS Nano* 8 (2014) 7229–7238.
- [17] J.B. Joo, I. Lee, M. Dahl, G.D. Moon, F. Zaera, Y. Yin, Controllable synthesis of mesoporous TiO₂ hollow shells: toward an efficient photocatalyst, *Adv. Funct. Mater.* 23 (2013) 4246–4254.
- [18] B. Bharti, S. Kumar, R. Kumar, Superhydrophilic TiO₂ thin film by nanometer scale surface roughness and dangling bonds, *Appl. Surf. Sci.* 364 (2016) 51–60.
- [19] G. Wang, Hydrothermal synthesis and photocatalytic activity of nanocrystalline TiO₂ powders in ethanol-water mixed solutions, *J. Mol. Catal. A-Chem.* 274 (2007) 185–191.
- [20] W. Shi, Grain-alignment Control Preparation of PMN-PT and BNT Piezoelectric Ceramics, Nanjing University of Technology, 2008.
- [21] C.M. Tank, Y.S. Sakhare, N.S. Kanhe, A.B. Nawale, A.K. Das, S.V. Bhoraskar, V.L. Mathe, Electric field enhanced photocatalytic properties of TiO₂ nanoparticles immobilized in porous silicon template, *Solid State Sci.* 13 (2011) 1500–1504.
- [22] C.A. Di, S. Xue, J. Tong, X. Shi, Study on electromechanical characterization of piezoelectric polymer PVDF in low-frequency band, *J. Mater. Sci. – Mater. Electron.* 25 (2014) 4735–4742.
- [23] S. Xu, G. Poirier, N. Yao, PMN-PT nanowires with a very high piezoelectric constant, *Nano Lett.* 12 (2012) 2238–2242.
- [24] E. György, A.P. Del Pino, A. Datcu, L. Duta, C. Logofatu, I. Iordache, A. Duta, Titanium oxide-reduced graphene oxide-silver composite layers synthesized by laser technique: wetting and electrical properties, *Ceram. Int.* 42 (2016) 16191–16197.
- [25] M. Conradi, A. Kocijan, Fine-tuning of surface properties of dual-size TiO₂ nanoparticle coatings, *Surf. Coat. Technol.* 304 (2016) 486–491.